Index Modulation for Frequency Diverse Array

Citation for published version:
Huang, G, Ouyang, S, Ding, Y & Fusco, V 2020, 'Index Modulation for Frequency Diverse Array', *IEEE Antennas and Wireless Propagation Letters*, vol. 19, no. 1, pp. 49-53.
https://doi.org/10.1109/LAWP.2019.2952576

Digital Object Identifier (DOI):
10.1109/LAWP.2019.2952576

Published In:
IEEE Antennas and Wireless Propagation Letters

Index Modulation for Frequency Diverse Array

Gaojian Huang, Shan Ouyang, Yuan Ding, *Member, IEEE*, and Vincent Fusco, *Fellow, IEEE*

***Abstract*—The Index Modulation (IM) approach adds an extra signal modulation dimension by utilizing sub-carrier index domain, that is in addition to the traditional IQ domain. Frequency diverse array (FDA) technology is rapidly developing as a new technique for radar systems. In this letter, a novel transmitter architecture for FDA, combining index modulation concept with FDA, namely IM-FDA, is presented. Compared with conventional frequency diverse arrays (CFDAs), the proposed architecture offers thumbtack-like beampatterns which can decouple the range and angle dependence, an issue existing in CFDA. An additional benefit is that apart from sensing target location, information can be conveyed to the targets through the selected frequency offset indices in the proposed scheme. The transmitter architecture is elaborated along with its design details and the efficacy of the proposed architecture is validated via numerical results for the transmit beampattern by comparison with CFDA and random frequency diverse array (RFDA).**

***Index Terms*—Frequency diverse array (FDA), index modulation frequency diverse array (IM-FDA), thumbtack-like beampattern**

I. INTRODUCTION

Frequency diverse array (FDA) methods have been of great interest in recent years in the radar community [1]–[8]. Unlike a phased array, in which all of the signals from radiating elements are modulated upon an identical radio frequency (RF) carrier subject to amplitude and phase weightings, in FDAs, a fraction of carrier frequency increment is applied across the array. This results in a time-range-angle dependent beampattern, which has the potential to resist interference in the range domain that is highly useful in radar sensing. However, inherent range-angle coupling is a problem associated with this method. Some works have been conducted to address this issue, such as using different types of small frequency offsets, e.g., [4]–[8]. In [4], a logarithmically increasing frequency offset FDA was proposed to achieve a single-maximum beampattern without periodic range variation, which was further extended in [5] by using multicarrier logarithmic frequency offset increments. Later, a concept using logarithmic frequency increments with a nonuniform spacing was proposed in [6] with suppressed sidelobes. In [7], a random frequency diverse array (RFDA) was introduced. In this study, each array element has a randomly assigned frequency offset that yields a thumbtack-like beampattern. Also, square (or cubic) increasing frequency offsets were proposed for the FDA, leading to an uncoupled range-angle beampattern [8], at the cost of larger operation bandwidth.

Sub-carrier index modulation was first proposed in [9], and orthogonal frequency division multiplexing index modulation (OFDM-IM) was suggested in [10]. The fundamental principle of OFDM-IM is an extension of two-dimensional (2-D) signal constellations (IQ plane for each subcarrier), with an additional dimension, which is the sub-carrier index dimension. This scheme provides a novel means of conveying information by mapping the data bits to the active sub-carrier indices. Thus, the information is conveyed not only by the M-ary signal constellations in IQ domains in each activated subcarrier, but also by the selected sub-carrier indices according to the baseband binary bits. The IM techniques for multiple input multiple output (MIMO) and multiple-carrier wireless systems were introduced in [11], suggesting a spectrum and energy efficient means for next generation communication systems.

In this letter, we report the first combination of IM techniques with frequency offset FDA. The proposed transmitter architecture provides a thumbtack-like beampattern, and the binary bits, being mapped to the selected frequency offset indices, can be conveyed to the target receiver as information bearers.

The paper is organized as follows. In Section II, the IM-FDA transmitter architecture and the associated system assumptions are first described, followed by the elaboration of its operation principle. In Section III, the radiated pattern simulations of the IM-FDA are presented and compared with those in CFDA/RFDA transmitters. Finally, Section IV concludes the letter.

II. PROPOSED IM-FDA

A. IM-FDA Transmitter

In this letter we consider a one-dimensional (1D) N-element linear FDA with uniform spacing d, see Fig. 1. The incoming D bits determine the activated frequency offset indices among all frequency offset indices allocated to the antenna elements. The selected frequency offset index set I_G is sent through the 'Antenna Frequency Mapping' module, which randomly assigns the selected frequency offset indices to each antenna element by way of closing the corresponding single-pole single-throw switches in the switch array. The signals then passed through a magnitude and phase control unit before feeding into their corresponding antenna elements. In this scheme, the excitation frequency of the n^{th} element can be expressed as

$$f_n = f_0 + m_n \Delta f U_{mn,q}(t) \tag{1}$$

where $n = 1, 2, \ldots, N$. f_0 is the reference carrier frequency in the order of GHz and Δf is a small frequency offset, which satisfies $\Delta f << f_0$. m_n is the frequency offset index of the n^{th} element, $m_n \in \{1, 2, \ldots, 2N\}$. $U_{mn,q}(t)$ in (1) refers to the on-off function in the time domain of the m_n^{th} switch for the n^{th} antenna element in the q^{th} symbol slot of duration T_s,

Mr. G. Huang's work was supported by the National Natural Science Foundation of China under Grant no.61871425, the Study Abroad Program for Graduate Student from Guilin University of Electronic Technology (GUET), China, and the Innovation Project of GUET Graduate Education.

G. Huang and S. Ouyang are with the School of Information and Communications, Guilin University of Electronic Technology, Guilin 541004, China (e-mails: gaojianhuang@yahoo.com and hmoysh@guet.edu.cn)

Y. Ding is with the Institute of Sensors, Signals and Systems (ISSS), Heriot-Watt University, Edinburgh EH14 4AS, U.K (e-mail: yuan.ding@hw.ac.uk)

V. Fusco is with the Institute of Electronics, Communications and Information Technology (ECIT), Queen's University of Belfast, Belfast BT3 9DT, U.K (e-mail: v.fusco@ecit.qub.ac.uk).

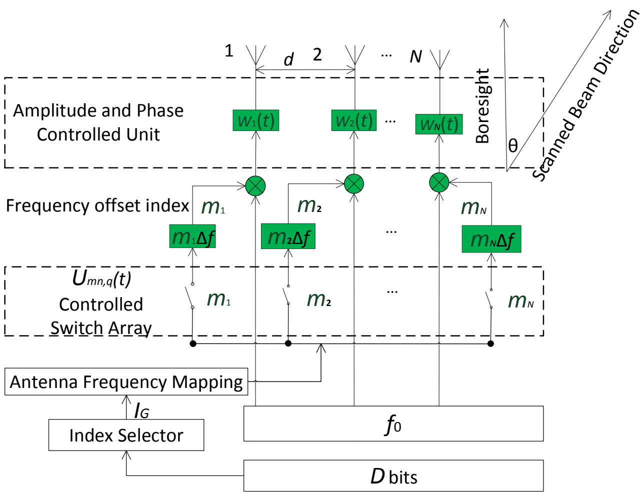

Fig .1. Proposed IM-FDA transmitter architecture.

$$U_{mn,q}(t)=\begin{cases}1 & qT_s\le t\le (q+1)T_s\\ 0 & otherwise\end{cases} \tag{2}$$

where '1' denotes 'on' state of the switch and '0' denotes 'off'. Here the switch is labeled corresponding to the frequency offset index - in other words, switch X routes the RF carrier with the frequency offset $X\Delta f$.

B. IM-FDA operation principle

In the proposed IM-FDA, I_G represents the selected frequency offset index sequence for the N array elements. For each transmitted D bits, N out of $2N$ frequency offsets are selected, and the selected frequency offset indices are

$$I_G=\{i_1, i_2, \ldots, i_g, \ldots, i_N\} \tag{3}$$

where $i_g\in\{1, 2, \ldots, 2N\}$, and $i_a\neq i_b$ when $a\neq b$. I_G is determined by the baseband data of D bits, where

$$D=\left\lfloor \log_2\left(C(2N, N)\right)\right\rfloor=\left\lfloor \frac{(2N)!}{N!N!}\right\rfloor \tag{4}$$

Here $C(2N, N)$ refers to the number of N-combinations out of a set of $2N$ elements and $N!$ denotes the factorial of N. Operator '$\lfloor\cdot\rfloor$' denotes integer floor function. The mapping procedures, from baseband D to N frequency offset indices, are now presented;

- The D bits are first converted to a decimal number c, using

$$c=\sum_{h=0}^{D-1}2^h D^{(h)} \tag{5}$$

  where $D^{(h)}$ represents the h^{th} bit in the D bit sequence. Here $0\le c\le C(2N, N)-1$;
- Next we map the decimal number c to a strictly decreasing sequence $\{j_N, j_{N-1}, \ldots, j_1\}$ by using the equation $c=C(j_N, N)+C(j_{N-1}, N-1)+\ldots+C(j_1, 1)$, wherein $j_a\in\{0, 1, 2, \ldots, 2N-1\}$, and $j_a\neq j_b$ when $a\neq b$; j_N is the largest natural number satisfying $C(j_N, N)\le c$. Note that in order to ensure one-to-one mapping between c and the sequence, the condition of strictly decreasing sequence has to be met, i.e., $j_N>j_{N-1}>\ldots>j_1$. In the case when $c=0$, $j_N=N-1$. Then, j_{N-l} is the natural number satisfying

$$C(j_{N-l}, N-l)\le c-\sum_{l=1}^{N-1}C(j_{N-l+1}, N-l+1)\le C(j_{N-l}+1, N-l) \tag{6}$$

- The sequence $\{j_N+1, j_{N-1}+1, \ldots, j_1+1\}$, termed as $\boldsymbol{J}$ hereafter, contains the selected frequency offset indices.

A one-to-one mapping between the D bits and the selected frequency offset indices $\boldsymbol{J}$ is guaranteed by the above mapping rule [10]. To better explain the mapping procedure, an example of $N=8$ is shown here. It is calculated using (4) that $D=\lfloor\log_2(C(16, 8))\rfloor=13$. If we assume, for example, the D bit sequence is '0 0 0 1 1 0 1 1 1 1 0 0 1', then using (5) we get the corresponding decimal number $c=889$. As $C(12, 8)=495<c=889<C(13, 8)=1287$, 12 is the largest number that satisfies the combinational numbers smaller than c. i.e., $j_8=12$. Similarly, via (6), j_7 to j_1 can be calculated, i.e., 11, 8, 7, 6, 2, 1 and 0, respectively. Therefore, the sequence $\boldsymbol{J}$ of {13, 12, 9, 8, 7, 3, 2, 1} contains the selected frequency offset indices, which is mapped from the information bits '0 0 0 1 1 0 1 1 1 1 0 0 1' by the 'Index Selector' module in Fig. 1. Hereafter, the selected frequency offset indices are randomly assigned to each radiating element. When the used frequency offset indices for each antenna element are known, the carrier frequency offsets are applied by closing the corresponding switches in the switch array, i.e., $U_{mn,q}(t)=1$.

C. Transmitted signal analysis

In the transmitter, we can write the radiated signal from the n^{th} element as

$$s_n(t)=W_n(t)e^{-j2\pi f_n t}\quad 0\le t\le T \tag{7}$$

where

$$W_n(t)=a_n e^{j\varphi_n}U_{mn,q}(t) \tag{8}$$

In (8), a_n and φ_n, respectively, represent the excitation amplitude and the initial phase at the time instant $t=0$. Here uniform amplitude is considered, namely $a_n=1$. In (7), T is transmitted pulse duration that is further divided into L equal sub-pulses of duration T_s. Here we assume a target is located at (R_1, θ) in free space with the first ($n=1$) antenna element taken as the range reference and the array boresight set as the angle reference. In one symbol duration, the received signal S of the target in far-field region can be expressed as

$$S(t; R_1, \theta)=\sum_{n=1}^{N}\frac{1}{R_n}s_n\left(t-\frac{R_n}{c_0}\right) \tag{9}$$

In (9) for the far-field assumption, when concerning only magnitude, the term $1/R_n$ is approximated as $1/R_1$, while concerning the phase, the term R_n/c_0 is substituted with $(R_1-(n-1)d\sin\theta)/c_0$, and c_0 is the speed of light. Substituting (1), (2), (7) and (8) into (9), S can be written as

$$S(t; R_1, \theta)=\frac{1}{R_1}e^{-j2\pi f_0\left(t-\frac{R_1}{c_0}\right)}\sum_{n=1}^{N}e^{j\varphi_n}\times e^{-j2\pi\left(m_n\Delta f t-\frac{m_n\Delta f R_1}{c_0}+\frac{(f_0+m_n\Delta f)(n-1)d\sin\theta}{c_0}\right)} \tag{10}$$

For (10), the corresponding array factor can be written as

$$AF\left(t;R_1,\theta\right)=\sum_{n=1}^{N}e^{j\varphi_n}\,\mathrm{e}^{-j2\pi\left(m_n\Delta ft-\frac{m_n\Delta fR_1}{c_0}+\frac{(f_0+m_n\Delta f)(n-1)d\sin\theta}{c_0}\right)} \tag{11}$$

In (11), m_n is random integer, selected from the sequence between 1 and $2N$. The term $e^{j\varphi_n}$ is used to steer the direction of the radiation peak. For instance, when $e^{j\varphi_n}$ is designed as

$$e^{j\varphi_n}=\mathrm{e}^{j2\pi\left(\frac{(f_0+m_n\Delta f)(n-1)d\sin\theta_X}{c_0}\right)} \tag{12}$$

the radiation pattern peak is steered to a target direaction at θ_X. Based on (11) and (12), the steered transmitting beampatttern of IM-FDA at the target direction θ_X can be given in (13)

$$B\left(t;R_1,\theta\right)=\left|\sum_{n=1}^{N}\mathrm{e}^{-j2\pi\left(m_n\Delta f\left(t-\frac{R_1}{c_0}\right)+\frac{(f_0+m_n\Delta f)(n-1)d(\sin\theta-\sin\theta_X)}{c_0}\right)}\right|^2 \tag{13}$$

III. Simulation and Analysis

In this section, the effectiveness of the proposed IM-FDA transmit beampattern is demonstrated by an example with the parameters listed in Table I. Here, $d = \lambda_{max} / 2.5$ where λ_{max} is the maximum wavelength of the electromagnetic waves radiated by the antenna array elements. When $N = 8$, it can be calculated that $D = 13$. In a single symbol duration T_s, assuming a bit stream of 13 bits is '0 0 0 0 0 0 0 0 0 1 1 1 0'. Following the mapping rules described in Section II, the selected frequency offset indices for the 8 antenna elements are {10, 8, 7, 6, 5, 4, 2, 1}. For fair comparison, the averaged beampatterns of the proposed IM-FDA and the RFDA with 10,000 Monte Carlo trials are plotted as the frequency offset applied to each element is randomly assigned for both the IM-FDA and the RFDA transmitters. It is noted that in each trial, the selected frequency offsets are determined by the incoming data, which are randomly and independently generated for the proposed IM-FDA. For RFDA, the frequency offset is a discrete random variable selected from $\{1\Delta f, 2\Delta f, 3\Delta f, \ldots, 2N\Delta f\}$, and the frequency offset assignment therefore follows a discrete uniform distribution. While, a linear increment frequency offset from $1\Delta f$ to $N\Delta f$ is used for the CFDA. All of the other parameters of these two transmitters are kept the same as the proposed IM-FDA example in Table I.

In Fig. 2(a), at a fixed time instant t = 0.1 ms, the normalized beampattern of range versus angle conveying the 13 bits binary information '0 0 0 0 0 0 0 0 0 1 1 1 0' to the target location (30 km, 20°) is shown. It can be seen that with the proposed scheme a thumbtack-shaped beampattern with most of the energy concentrated at the location (30 km, 20°) being achieved. In Fig. 2(b), a coupled range-angle beampattern for CFDA is shown, suggesting that the targets' range information cannot be directly obtained from the beampattern peak, meanwhile, multiple maxima in the beampattern weakens the capability for interference rejection. By contrast, the proposed IM-FDA provides only a single beampattern peak in concerned area. In Fig. 2(c), the averaged beampattern of the IM-FDA exhibits a thumbtack-like shape at (30 km, 20°). Compared with the beampattern of the RFDA in Fig. 2(d), a lower energy distribution along the target direction in the range domain is achieved. This can be explained by the frequency offset distributions. The example RFDA can randomly select the frequency offsets from $1\Delta f$ to $16\Delta f$ for each element with possible repetition, while for the proposed IM-FDA, the

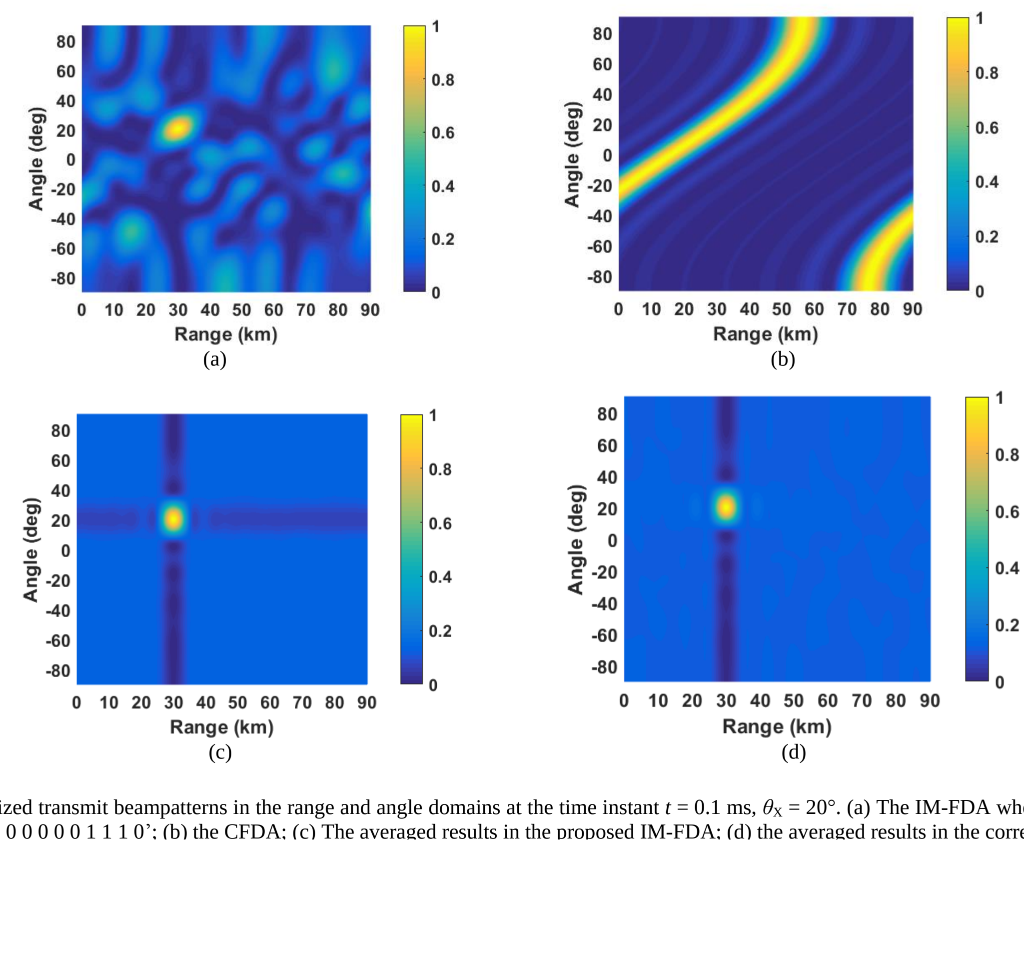

Fig. 2. Normalized transmit beampatterns in the range and angle domains at the time instant t = 0.1 ms, θ_X = 20°. (a) The IM-FDA when transmitting a bit sequence '0 0 0 0 0 0 0 0 0 1 1 1 0'; (b) the CFDA; (c) The averaged results in the proposed IM-FDA; (d) the averaged results in the corresponding RFDA.

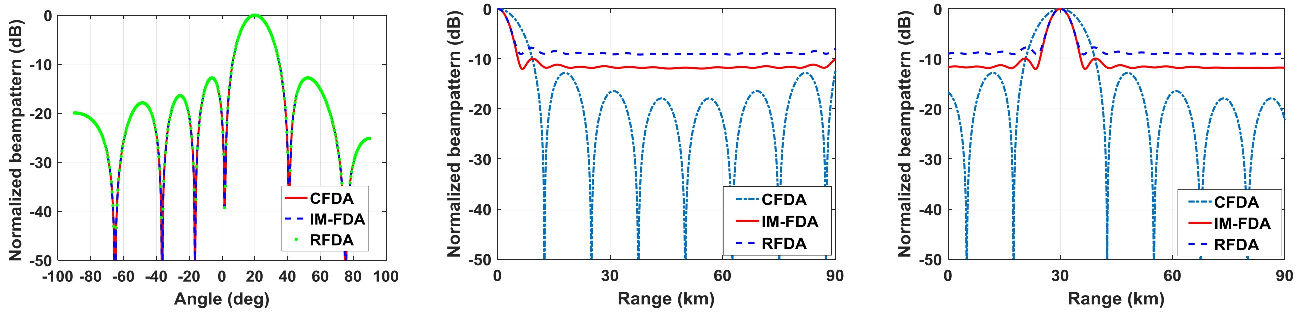

(a) (b) (c)

Fig. 3. (a) Normalized beampattern in the angle domain for the CFDA, the proposed IM-FDA and the RFDA, at t = 0.1 ms, R_1 = 30 km; (b) Normalized beampattern in the range domain for the CFDA, the proposed IM-FDA, and the RFDA, at t = 0 ms, θ_X = 20°; (c) Normalized beampattern in the range domain for the CFDA, the proposed IM-FDA, and the RFDA, at t = 0.1 ms, θ_X = 20°.

TABLE I

EXAMPLE IM-FDA TRANSMITTER PARAMETERS

Parameters	**Values**
N	8
f_0	8 GHz
Δf	3 kHz
d	0.015 m
m_n	1, 2, …, 16
T_s	0.1 ms
T	0.3 ms

frequency offset of each element can only be uniquely selected from 1Δf to 16Δf. Meanwhile, we observe that the similar shapes of the desired energy focusing points are achieved in the RFDA and the proposed IM-FDA schemes. For the proposed IM-FDA and the RFDA, the similar fields around the target location in the range domain can be explained by the similar signal bandwidth adopted in both schemes. Note that in Figs. 2(c) and (d), the total transmit energy is equal for the IM-FDA and the RFDA. In the IM-FDA the suppressed sidelobe energy along the target direction is redistributed in the non-target directions in the range domain. For example, comparing Fig. 2(d) with Fig. 2(c), in the RFDA the energy distribution along a non-target direction of 40° is approximately 0.2 dB lower than that in the IM-FDA scheme. When considering the detection, the sidelobe suppression of 3 dB along the target direction is likely to overweigh the marginal increase of the background noise.

For better comparison and illustration, in Fig. 3(a), the angle responses at R_1 = 30 km are depicted. It is shown that the CFDA, the proposed IM-FDA and the RFDA schemes achieve the same side lobe levels in the angle domain. While, Fig. 3(b) and (c) show the range responses of these three schemes for different time instants along a fixed target direction. It can be seen that the proposed IM-FDA and the RFDA schemes have higher range resolutions. This is due to the larger bandwidths used in these two schemes. In the IM-FDA the energy distributions traveling along the distance, at the target direction θ_X = 20°, are approximately 3 dB lower than that in the RFDA scheme. This indicates that the proposed IM-FDA scheme is more capable of rejecting range-dependent interference than the RFDA scheme. When comparing the range responses among these three transmit beampatterns, it can be concluded that the CFDA has the lowest side lobe levels because of the linearly increasing frequency offsets.

IV. Conclusion

In this letter, a transmitter concurrently using IM and FDA techniques was proposed. In the proposed scheme, incoming data bits are systematically mapped to the selected frequency offset indices adopted by each element. It has been shown that the proposed scheme achieves a thumbtack-like transmit beampattern with only a single beampattern peak at the target location, enabling the capability of decoupling the range-angle that exists in the CFDA beampatterns. In addition, information bits can be transmitted to the targets by exploiting the transmitted frequency offset indices, indicating that the proposed scheme can deliver wireless communication and radar sensing simultaneously.

References

[1] P. Antonik, M. C. Wicks, H. D. Griffiths, and C. J. Baker, "Frequency diverse array radars," in *Proc. IEEE Radar Conf.*, Verona, NY, USA, Apr. 2006, pp. 215–217.

[2] M. Secmen, S. Demir, A. Hizal, and T. Eker, "Frequency diverse array antenna with periodic time modulated pattern in range and angle," in *Proc. IEEE Radar Conf.*, Boston, MA, USA, Apr. 2007, pp. 427–430.

[3] P. F. Sammartino, C. J. Baker and H. D. Griffiths, "Frequency diverse MIMO techniques for radar," *IEEE Trans. Aerosp. Electro. Syst.*, vol. 49, no. 1, pp. 201–222, Jan. 2013.

[4] W. Khan, I. M. Qureshi, and S. Saeed, "Frequency diverse array radar with logarithmically increasing frequency offset," *IEEE Antennas Wireless Propag. Lett.*, vol. 14, pp. 499–502, 2015.

[5] H. Shao, J. Dai, J. Xiong, H. Chen, and W. Wang, "Dot-shaped range-angle beampattern synthesis for frequency diverse array," *IEEE Antennas Wireless Propag. Lett.*, vol. 15, pp. 1703–1706, 2016.

[6] M. Mahmood and H. Mir, "Frequency diverse array beamforming using nonuniform logarithmic frequency increments," *IEEE Antennas Wireless Propag. Lett.*, vol. 17, no. 10, pp. 1817–1821, Oct. 2018.

[7] Y. Liu, H. Ruan, L. Wang, and A. Nehorai, "The random frequency diverse array: a new antenna structure for uncoupled direction-range indication in active sensing," *IEEE J. Sel. Topics Signal Process.*, vol. 11, no. 2, pp. 295–308, March. 2017.

[8] K. Gao, W. Wang, J. Cai, and J. Xiong, "Decoupled frequency diverse array range-angle-dependent beampattern synthesis using non-linearly increasing frequency offsets," *IET Microw. Antennas Propag.*, vol. 10, no. 8, pp. 880–884, 2016.

[9] R. Abu-alhiga and H. Haas, "Subcarrier-index modulation OFDM," in *Proc. IEEE Int. Sym. Personal, Indoor,Mobile Radio Commun.*,Tokyo, Japan, Sep. 2009, pp. 177–181.

[10] E. Başar, Ü. Aygölü, E. Panayırcı, and H. V. Poor, "Orthogonal frequency division multiplexing with index modulation," *IEEE Trans. Signal Process.*, vol. 61, no. 22, pp. 5536–5549, Nov. 2013.

[11] E. Basar, "Index modulation techniques for 5G wireless networks," *IEEE Commun. Mag.*, vol. 54, no. 7, pp. 168–175, July. 2016.